catalysts

MDPI

Review

Bismuth Vanadate ($BiVO_4$) Nanostructures: Eco-Friendly Synthesis and Their Photocatalytic Applications

Hajar Q. Alijani [1], Siavash Iravani [2,*] and Rajender S. Varma [3,*]

[1] Department of Biotechnology, Shahid Bahonar University of Kerman, Kerman 7616913439, Iran
[2] Faculty of Pharmacy and Pharmaceutical Sciences, Isfahan University of Medical Sciences, Isfahan 8174673461, Iran
[3] Regional Centre of Advanced Technologies and Materials, Czech Advanced Technology and Research Institute, Palacký University in Olomouc, Šlechtitelů 27, 783 71 Olomouc, Czech Republic
* Correspondence: siavashira@gmail.com (S.I.); varma.rajender@epa.gov (R.S.V.)

Abstract: Green nanotechnology plays an important role in designing environmentally-benign and sustainable synthesis techniques to provide safer products for human health and environments. In this context, the synthesis of bismuth vanadate ($BiVO_4$) nanoparticles (NPs) based on green chemistry principles with the advantages of eco-friendliness, cost-effectiveness, and simplicity has been explored by researchers. Despite the advantages of these synthesis techniques, crucial aspects regarding their repeatability and large-scale production still need to be comprehensively explored. $BiVO_4$ NPs have shown excellent potential in the pharmaceutical industry, cancer therapy, and photocatalysis. $BiVO_4$ particles with monoclinic scheelite structures have been widely investigated for their environmental applications owing to their fascinating optical and electrical properties as well as their high stability and unique crystal structure properties. These NPs with good photostability and resistance to photocorrosion can be considered as promising nanophotocatalysts for degradation of pollutants including organic dyes and pharmaceutical wastes. However, additional explorations should be moved toward the optimization of reaction/synthesis conditions and associated photocatalytic mechanisms. Herein, recent developments regarding the environmentally-benign fabrication of $BiVO_4$ NPs and their photocatalytic degradation of pollutants are deliberated, with a focus on challenges and future directions.

Keywords: bismuth vanadate ($BiVO_4$) nanoparticles; green chemistry; plant-mediated biosynthesis; photocatalytic applications; photocatalytic degradation; pollutants

check for updates

Citation: Q. Alijani, H.; Iravani, S.; Varma, R.S. Bismuth Vanadate ($BiVO_4$) Nanostructures: Eco-Friendly Synthesis and Their Photocatalytic Applications. *Catalysts* **2023**, *13*, 59. https://doi.org/10.3390/catal13010059

Academic Editors: Collin G. Joseph, Gianluca Li Puma, Giovanni Palmisano and María Victoria López Ramón

Received: 20 November 2022
Revised: 13 December 2022
Accepted: 25 December 2022
Published: 28 December 2022

1. Introduction

Bismuth is a brittle white metal with a pink undertone and a rainbow matte that tarnishes yellow to dark gray. This diamagnetic metal has a hall effect. Accordingly, it has low electrical conductivity with stable electronic configuration, containing three electrons in the 6p orbital, along with high electrical resistance in a magnetic field. The most important ores of this element are bismuthinite (Bi_2S_3) and bismite (Bi_2O_3) [1,2]. Bismuth has many applications in industry and biomedicine [3,4]. For instance, bismuth subsalicylate ($C_7H_5BiO_4$), under the brand name Pepto-bismol, is a colloidal drug used to treat the gastrointestinal diseases. Bismuth oxychloride (BiOCl) is a lustrous white powder that makes cosmetics shine. Bismuth compounds are also used in the production of synthetic fibers, rubber, nuclear reactors, transuranium elements, metal alloys, supercapacitor [5], among others [6]. Bismuth vanadate ($BiVO_4$) is a yellow mineral solid that has garnered a lot of attention in recent years as a nanocatalyst. $BiVO_4$ has three polymorphism structures—$BiVO_4$ with reddish/yellowish brown color has a natural polymorph called pucherite with orthorhombic crystal system, and the other two polymorphs of $BiVO_4$ are clinobisvanite and dreyerite. Clinobisvanite is an orange polymorph of $BiVO_4$ with a monoclinic scheelite crystal system. The clinobisvanite bismuth vanadate often forms pseudo-tetragonal crystals, including

tetragonal scheelite. The rarest polymorph of $BiVO_4$ is dreyerite, the orange/brownish-yellow material with tetragonal zircon crystal system. However, monoclinic clinobisvanite is an excellent light-driven photocatalyst compared to other polymorphs [7–9].

The synthesis of $BiVO_4$ nanoparticles (NPs) has been performed using different methods, namely sol-gel [10], hydrothermal technique [7], reverse-micro emulsion technique, co-precipitation [11], sonochemical [12,13], and solvothermal [14], among others [15]. The unique optical, electrical, catalytic and biocompatibility properties of $BiVO_4$ NPs depend on their crystal structure. Meanwhile, green nanotechnology can be applied for developing eco-friendly preparative techniques for synthesizing nanomaterials with the advantages of cost-effectiveness, low toxicity, biocompatibility, and eco-friendly properties [16–20]. On the other hand, a wide variety of nanophotocatalysts such as ZnO, TiO_2, Fe_2O_3, CdS, and ZnS have been deployed for environmental applications (especially photocatalytic degradation of pollutants), showing unique chemical, electrical, optical and physical features [21–24]. Among these, $BiVO_4$ NPs with excellent photostability and resistance to photocorrosion can be considered as attractive photocatalysts for degradation of pollutants including organic dyes and pharmaceutical wastes [24,25]. Additionally, these NPs with the benefits of non-toxicity and eco-friendliness have displayed suitable antibacterial effects, making them potential candidates for environmental purposes [26]. In this context, designing composites containing $BiVO_4$ NPs and other materials such as nickel ferrite ($NiFe_2O_4$) can help improve their photocatalytic features, thus enhancing the absorption region for efficiently degradation of pollutants [27]. For instance, $BiVO_4/NiFe_2O_4$ composites were fabricated for the photodegradation of methylene blue under visible light. Accordingly, these composites could efficiently degrade methylene blue (~99%) after 90 min under visible light [28]. Lee et al. [29] reported the synthesis of copper (Cu)-doped $BiVO_4$/graphitic carbon nitride (g-C_3N_4) nanocomposites with improved stability, light-harvesting efficiency, and electron/hole (e−/h+) pair separation compared to pristine g-C_3N_4 and $BiVO_4$, showing enhanced photocatalytic performance [29]. Herein, the most recent advancements pertaining to the eco-friendly synthesis of $BiVO_4$ NPs and their photocatalytic applications are cogitated, focusing on important challenges and future perspectives.

2. Eco-Friendly Synthesis of $BiVO_4$ NPs

2.1. Biosynthesis Techniques

Biosynthesis of NPs is based on the employment of biological resources for the synthesis without the use of organic or inorganic chemicals as reducing and stabilizing agents (Table 1) [24,30]. However, crucial challenges such as the polydispersity of NPs, size/morphology controllability, and commercial/large-scale production of NPs still linger [31,32]. According to the literature, plant phytochemicals and some primary metabolites such as polyphenols, flavonoids, glycosides, tannins, proteins, terpenoids, and polysaccharides have a reducing, coating and stabilizing role in the synthesis of NPs [33–36]. In addition, each of these plant constituents has therapeutic properties; the multiple roles of plant compounds in green synthesis have garnered much attention lately where flavonoids and phenolic compounds have played a key role in the synthesis of $BiVO_4$ NPs. The diol and hydroxyl functional groups in phenolic compounds and flavonoids reduce the metal ions [37]. It has been well established that flavonoid, terpenoids, antioxidants, and phenolic compounds could play an important role in the synthesis of $BiVO_4$ NPs; largely free functional group in these phytochemicals being hydroxyl (OH) performing a crucial function in coating and reducing the metal ions in the biosynthesis of $BiVO_4$ NPs [37,38].

Table 1. Some selected examples of $BiVO_4$ NPs synthesized using eco-friendly techniques.

Salts	Chelating Agents	Crystal Structure	Shape of NPs	Plant Phytochemicals	Applications	Refs.
$Bi(NO_3)_3$ and $VOSO_4$	Flower extract of *Callistemon viminalis* (bottlebrush)	Monoclinic scheelite	Nanorods (the basal and longitudinal dimensions of the nanorods ranged from 350 to 450 nm and 1.2–2 µm, respectively)	Flavonoids, saponins, alkaloids, steroids and triterpenoids	Photocatalytic activity (methylene blue)	[39]
NH_4VO_3 and $Bi(NO_3)_3$	Fruit extract of *Unripe jackfruit*	Monoclinic scheelite	The asymmetrically arranged $BiVO_4$ nanostructures (the shapes were nearly spherical and hexagonal); the size being ~90–250 nm	Carotenoids, flavonoids, volatile acids sterols and tannins stilbenoids, and arylbenzofurons	Anticancer (breast cancer cell lines), Photocatalytic activity (Methylene blue) and electrochemical sensor	[40,41]
-	*Citrus Limon* (lemon)	Pure monoclinic	Flower-like structures	Citric acid	Photocatalytic activity (Indigo Carmine) and electrochemical sensor	[42]
$Bi(NO_3)_3$ and $VOSO_4$	Fruit extract of *Hyphaene thebaica*	Clinobisvanite monoclinic	Nanorods (well-aligned rod shaped)	Cinnamic acid, flavonoids, vanillic acid, epicatechin, glycosides, stilbene and sugars composition	Antibacterial, antifungal, and antiviral activity	[43,44]
NH_4VO_3 and $Bi(NO_3)_3$	Fruit extract of *Aegle marmelos* (bael)	Monoclinic scheelite	-	Flavonoids, polyphenols tannins, alkaloids, coumarins, steroids and natural sugar	Antibacterial, antifungal, and photocatalytic activity (methylene blue)	[38,45]

The size of $BiVO_4$ nanorods increased with the rise in the calcination temperature of NPs [39]; calcination of $BiVO_4$ NPs eliminated the elemental and plant impurities. The crystallinity of $BiVO_4$ NPs was decreased by tripling the amount of plant precursor. However, the antibacterial and antifungal activity of the NPs was increased while tripling the plant precursor [38]. The increase in plant precursor has led to the formation of bulk $BiVO_4$ and distortion of the symmetry of the tetrahedron structure to the hexagonal of $BiVO_4$ NPs. This increase could also enhance the absorption of electric charge, cavities and photocatalytic activity of $BiVO_4$ NPs. These NPs exhibited efficient photocatalytic performance owing to their remarkable separation rate of photodegraded charge carriers, causing the degradation up to 98.3% under visible light irradiation for 120 min [41]. On the other hand, $BiVO_4$ NPs containing these plant precursors had the highest inhibitory properties against MCF-7 cancer cells. Accordingly, the calcination and the amounts of plant extracts affect the crystal structure, purity, and photocatalytic and medicinal activity of $BiVO_4$ NPs [41].

2.2. Microwave- and Ultrasonic-Assisted Synthesis

Microwave (MW)-assisted synthesis techniques have shown several advantages of cost-effectiveness, simple/time-saving purification, eco-friendliness, and fast reaction times [46,47]. These methods with significant reactivity, rapid heating, and non/low pollutions can be contemplated for safer synthesis of $BiVO_4$ nanomaterials, reducing the energy and time consumption [48]. Spherical hollow $BiVO_4$ nanocrystals with good optoelectronic properties were fabricated using MW-assisted combustion synthesis technique with the

advantages of low energy consumption, rapidness, and simplicity. These NPs could be employed for the photocatalytic degradation of Alizarin Red S pollutant (~99.6%) after 180 min at natural pH. After the pore structure analysis, it was revealed that the lowest pore diameter of $BiVO_4$ nanocrystals was ~4.41 nm. The synthesis routes and conditions can significantly affect the size and size distribution of these nanomaterials [49]. Tungsten (W)-doped $BiVO_4/WO_3$ heterojunctions were constructed using one-pot MW-assisted technique within 24 min. These heterojunctions exhibited improved photocatalytic performance and increased photogenerated charges lifetime, wherein W doping could reduce the recombination rates [50]. In addition, monoclinic $BiVO_4$ structures were synthesized via a facile and rapid combined MW- and ultrasonic irradiation protocol to provide photocatalysts for the degradation of Rhodamine B under visible light irradiation. These NPs with a small crystal size and large band gap displayed excellent photocatalytic activity [51].

Souza et al. [52] synthesized $BiVO_4$ nanoflowers decorated with gold (Au) NPs using MW irradiation. In these nanostructures, $BiVO_4$ exhibited low band gap energy under visible light irradiation and Au NPs could serve as electron sinks and/or as electron sources via plasmon resonance, enhancing the charge separation of photogenerated electrons and holes. These photocatalysts with synergistic effects could be applied for the degradation of methylene blue (~95%) after 6 h under UV–visible light irradiation [52]. In addition, pure monoclinic $BiVO_4$ NPs (~50 nm) were synthesized using a single-step, pH-controlled, MW-assisted technique at a temperature of 90 °C within a short reaction time (60 min) [53]. The introduced synthesis strategy can be considered as an up-scalable, low-temperature, and environmentally-benign alternative after the optimization of crucial factors such as pH, temperature, and reaction time controlling the morphology and crystal phase. These NPs could be applied for the photodegradation of Rhodamine B [53]. Despite the advantages of MW-assisted synthesis such as reduction in time and energy consumptions, the specific interaction of the microwaves with the reactive species is one of the important challenging issues. Notably, controlling the morphology and size of nanomaterials is another crucial aspect that needs suitable optimization of reaction conditions [54]. In ultrasonic-assisted synthesis of $BiVO_4$ photocatalysts, it was revealed that ultrasonic irradiation time could affect the relevant features of visible-light-driven $BiVO_4$ [55]. Notably, after the optimization of synthesis conditions, the enhanced photocatalytic activity could be obtained as exemplified in one study for the ultrasonic-assisted synthesis of $BiVO_4$ photocatalysts with 60% pollutant degradation within 40 min of ultrasonic irradiation [55].

3. Photocatalytic Applications

Photocatalysts are semiconductor catalysts that absorb photons of light to create an electron–hole pair. Some important applications of semiconductor photocatalytic materials include:

- Degradation of organic pollutants in industrial effluents,
- Water treatment (the removal of stable organic compounds and microorganisms from municipal and laboratory wastewater),
- Air purifier,
- Paper industry,
- Disinfection of surgical instruments, and
- The removal of fingerprints from electrically and optically sensitive components.

$BiVO_4$ NPs can be deployed for the photocatalytic hydrogen evolution and dye degradation [56]. Overall, ternary metal oxide nanomaterials have shown excellent photocatalytic abilities, since their electronic bands are generated by atomic orbitals of more than one element and the inflection of the stoichiometric ratio of the elements can superbly adjust the band gap energy and capabilities of valence and conduction bands [49]. $BiVO_4$ as a direct band gap ternary metal oxide semiconductor with a band gap of 2.4 eV for solar light absorption can be deployed for photocatalytic applications. Because the conduction band exists closely to the empty Bi 6p orbitals, its overlap with the anti-bonding V 3d, O 2p states can additionally diminish the requirement for external bias for photocatalytic activity. In

this context, the charge transport and interfacial charge transfer are crucial challenges in its performance [49,57]. $BiVO_4$ photocatalysts can be employed for water oxidation owing to small band gap and appropriate band positions; however, for practical applications, short diffusion length should be resolved [58]. For instance, $BiVO_4/BiO_x$ composites with long-term stability were prepared on conducting glasses through a hydrothermal fabrication technique and NaOH etching process, with improved photoelectrochemical catalytic capabilities towards water oxidation [58]. In addition, $BiVO_4$ nanocatalysts were synthesized for the elimination of toxic organic pollutants from wastewater, electrochemical storage, and photoelectrochemical solar water oxidation. These NPs exhibited excellent photocatalytic performance for the degradation of methyl orange under visible light (~87.8%) within 80 min [59].

Heterogeneous photocatalysis has been performed for the degradation of organic dyes (Rhodamine 6G) using $BiVO_4$ thin films under visible light irradiation. The sputtered $BiVO_4$ films displayed an electronic band gap of 2.5 eV, making them suitable candidates for harvesting the visible light radiation [15]. In addition, monoclinic BiVO4 NPs (~50–70 nm) were synthesized for efficient visible light photocatalytic degradation of Rhodamine B and crystal violet as they exhibited improved photocatalytic performance for the degradation of pollutants under visible light [60]. $BiVO_4$ NPs calcined at 400 °C exhibited excellent photocatalytic activity against methylene blue dye under solar irradiation, displaying good stability (~3 cycles) [61]. These photocatalysts could also be applied for the inhibition of pathogenic bacteria such as *Pseudomonas aeruginosa*, *Acinetobacter baumannii*, and *Staphylococcus aureus*. The suggested antibacterial effects of these photocatalysts included the bacterial cell wall damages, the disruption of DNA replications and bacterial metabolisms, the inhibition of formation of proteins, and the reactive oxygen species (ROS) [61]. Sharma et al. [62] fabricated monoclinic $BiVO_4$ nanomaterials with suitable antimicrobial and photocatalytic performances. These nanostructures exhibited photocatalytic degradation efficiency towards methylene blue pollutant, along with the efficient antibacterial effects against *Escherichia coli* (Figure 1) [62].

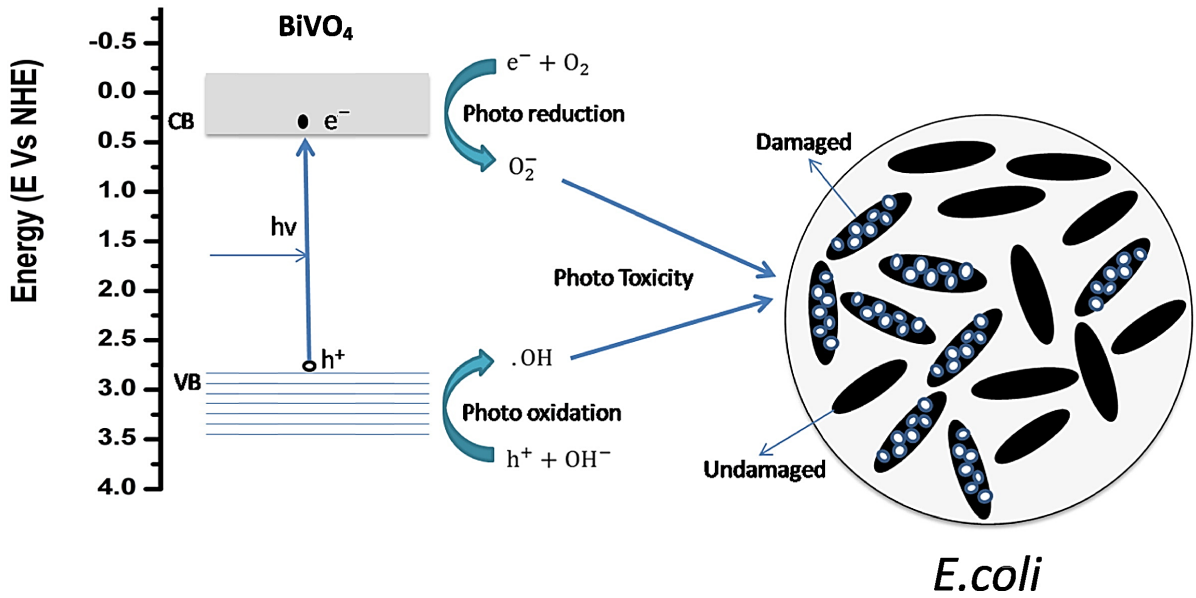

Figure 1. The mechanism of antibacterial effects of monoclinic $BiVO_4$ nanomaterials against pathogenic bacteria. Adapted from [62] with permission. Copyright 2016 Elsevier.

$BiVO_4$ NPs can be considered as light-driven photocatalysts due to their ferroelasticity, optical, and conductive nature [63]. These NPs have been deployed to remove phenolic compounds, methyl orange, methylene blue, and indigo carmine (Table 2). The photocatalytic performance of these NPs depends on the band structure of the electron, crystal

structure, and their band gap energy. For an efficient photocatalyst, the gap band energy must be less than 3 eV to exploit light absorption in the visible region to utilize solar energy efficiently. Indirect and direct mechanisms as well as the photosensitization processes are effective in the photodegradation of pollutants [63]. According to the literature, the band gap energy caused the molecular excitation of the $BiVO_4$ photocatalysts. Molecular excitation generates electrons in the higher conduction band (Ecb) and positive holes in the lower capacitance band (Evb) energies in $BiVO_4$. The electron hole (h+) causes oxidative processes and traps e− for reduction processes; also, the formation of superoxide anion and hydrogen peroxide can be obtained from oxygen. During the photocatalytic oxidation processes, pollutants are completely degraded by ultraviolet radiation in the presence of $BiVO_4$ catalysts and converted to CO_2 and H_2O. $BiVO_4$ photocatalysts with environmental and energy applications have shown efficient light activation, high stability, low cost, and safety advantages for the environment and humans. In one study, $BiVO_4$/graphene oxide/polyaniline composites were synthesized for photodegradation of methylene blue and safranin O upon the covering of polyaniline. The improvement in their photocatalytic performances was due to the formation of well-defined composite interfaces enhancing the charge separation efficacy [64].

Table 2. Selected examples of photocatalytic degradation of pollutants using biosynthesized $BiVO_4$ NPs under visible light irradiation.

Shape and Crystal Structure of NPs	Plant Extracts	Pollutants	Degradation Efficiency (%)	Absorption Peak (nm)	Gap Band (eV)	Refs.
Monoclinic scheelite and nanorods	*Callistemon viminalis*	Methylene blue	82.63	661	2.59	[39]
Monoclinic scheelite	*Aegle marmelos*	Methylene blue	90	663	2.5	[38]
Monoclinic scheelite and quasispherical-like structure	*Unripe jackfruit*	Methylene blue	98.3	250–300	2.4	[41]
Flower-like and monoclinic scheelite	*Citrus Limon*	Indigo Carmine	90.6	610	∼2.6–2.8	[42]

Tahir et al. [65] constructed ternary WO_3/g-C_3N_4@$BiVO_4$ composites through an eco-friendly hydrothermal technique for the efficient production of hydrogen energy. These composites with active sites for photocatalytic reduction of water exhibited improved photocatalytic performance (432 μmol $h^{-1}g^{-1}$), offering great opportunities for energy harvesting. $BiVO_4$ NPs with unique optical properties and photocatalytic performance could inhibit the recombination of photogenerated electron and holes and enhance the reduction reactions for H_2 formation. The enhancement in photocatalytic efficiency of these photocatalysts could be due to the large surface area, efficient separation of electrons/holes pairs, and wide absorption region of visible light, because of the synergistic influences between WO_3/g-C_3N_4 and $BiVO_4$ NPs [65]. $BiVO_4$ photocatalysts with low band gap energy have been applied for eco-friendly and sustainable H_2O_2 generation [66]. $BiVO_4$ nanostructures were encapsulated with encapsulated for photocatalytic H_2O_2 formation; reduced graphene oxide was deployed for the stimulation of transporting charges and prevention of recombining photogenerated electron–hole pairs (Figure 2) [66]. The photocatalysts displayed efficient formation of H_2O_2 using oxalic acid, stimulating two-electron O_2 reduction reaction with suitable cyclic stability; the photocatalytic flow reactor evaluation was applied for assessment of the feasibility of continuous generation of H_2O_2 [66].

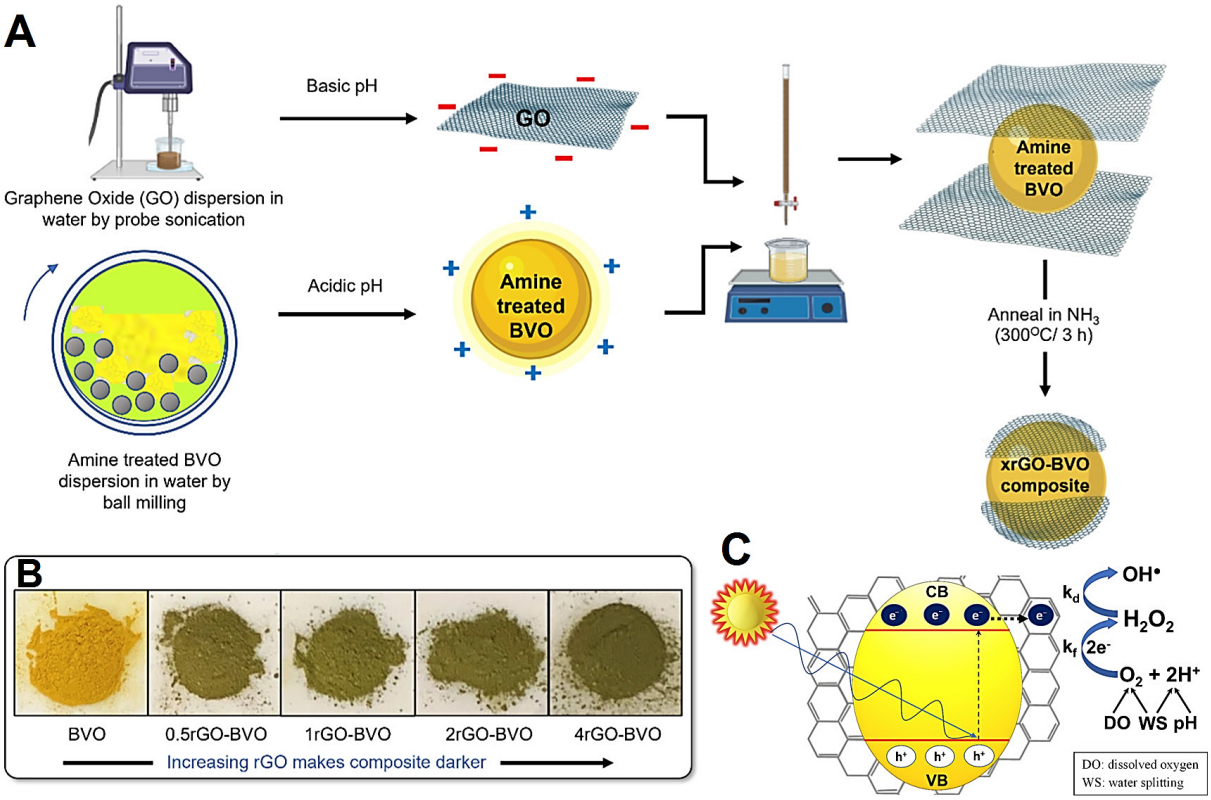

Figure 2. (**A**) The encapsulation of $BiVO_4$ (BVO) with reduced graphene oxide (rGO). (**B**) Digital photographs of the commercial BVO and the prepared composites. (**C**) Mechanism of photocatalytic generation of H_2O_2. Adapted from [66] with permission. Copyright 2021 American Chemical Society.

$BiVO_4$ nanophotocatalysts synthesized by an ultrasonic-assisted synthesis technique were deployed for photocatalytic degradation of organic dyes under visible light irradiation [67]. Besides, $BiVO_4$ photocatalysts were applied for the photodegradation of Rhodamine B and 2,4-Dichlorophenol [68]. It was revealed the photocatalysts exhibited high photocatalytic performance at pH = 7 for 24 h for the photodegradation of Rhodamine B, while the best photodegradation of 2,4-Dichlorophenol could be achieved at pH = 0.5 for 24 h. Accordingly, the photocatalytic mechanism could be proposed by various charge carrier transfer pathways and active oxidation species in the heterostructured $BiVO_4$ photocatalysts [68]. Similarly, monoclinic $BiVO_4$ structures were investigated for the photocatalytic degradation of methyl orange under visible light irradiation [69]. The pH value could significantly affect the pore structure and morphology of these nanomaterials. As a result, spherical $BiVO_4$ with porous structures along with the flower-cluster-like and flower-bundle-like $BiVO_4$ structures were prepared at different pH levels. Notably, some important criteria such as surface area, bandgap energy, surface oxygen vacancy density, and porous architectures could highly affect the photocatalytic performance of these catalysts [69]. Several studies have focused on the related mechanisms of photocatalytic reactions by these photocatalysts which can help to enhance the catalytic efficiency for future practical applications [70]. Remarkably, noble metals can be deposited on the surface of $BiVO_4$ for improving the photocatalytic efficiency by functioning as an electron trap because of the generation of the Schottky barrier, thereby decreasing the electron–hole recombination procedure. In one study, after the synthesis of Pt-$BiVO_4$ catalysts, analysis was performed on trapping reactive oxygen species ($^{\bullet}OH$ and $^{\bullet}O_2^{-}$). As a result, the radicals like $^{\bullet}OH$ were generated on the surface of semiconductor as a robust oxidizing agents, which could attack the adsorbed organic molecules and participate in additional oxidation procedure [70]. Additionally, the study on dynamic of photogenerated holes in $BiVO_4$ photoanodes for solar water oxidation revealed that two different recombination

procedures limited the photocurrent formation in $BiVO_4$ photoanodes, which included the recombination of surface-accumulated holes with bulk $BiVO_4$ electrons along with the rapid electron/hole recombination [71].

In addition to photodegradation of dye pollutants, $BiVO_4$ structures can be considered as promising alternatives for efficient degradation of pharmaceutical wastes [72]. For instance, spindle-shaped $BiVO_4$/reduced graphene oxide/g-C_3N_4 nanocomposites with excellent solar-driven degradation activity were constructed as Z-scheme photocatalysts for the degradation of antibiotics (Figure 3) [73]; the photodegradation rates were ~81.10% and ~94.8% for tetracycline and ciprofloxacin in 60 min, respectively. These photocatalysts exhibited oriented carrier transport, photooxidation response, and superb optical activity, showing enhanced photogenerated electron–hole pairs and rapid carriers transfer under visible-light irradiation [73]. To design photocatalysts with improved photodegradation efficiency toward ciprofloxacin, the hybrid reduced graphene oxide-$BiVO_4$ composite was designed using a facile MW-assisted synthesis technique [72]. Compared to the pure $BiVO_4$ photocatalysts, this photocatalyst exhibited enhanced photodegradation capability toward ciprofloxacin under visible light. The composite displayed the highest ciprofloxacin degradation ratio (~68.2%) in 60 min, which was over three times than that (~22.7%) observed for pure $BiVO_4$ photocatalysts. This enhancement in photocatalytic potential was due to the effective separation of electron–hole pairs rather than the increase in light absorption [72]. In another study, $BiVO_4$ nanophotocatalysts with high recycling potential were synthesized for the removal of tetracycline and oxytetracycline antibiotics [74]. Accordingly, excellent performance of 72% and 83% degradation could be attained after 240 min under sunlight conditions for tetracycline and oxytetracycline, respectively. Mechanism studies revealed that the photogenerated electrons and holes could play crucial roles in the elimination of these pollutants [74].

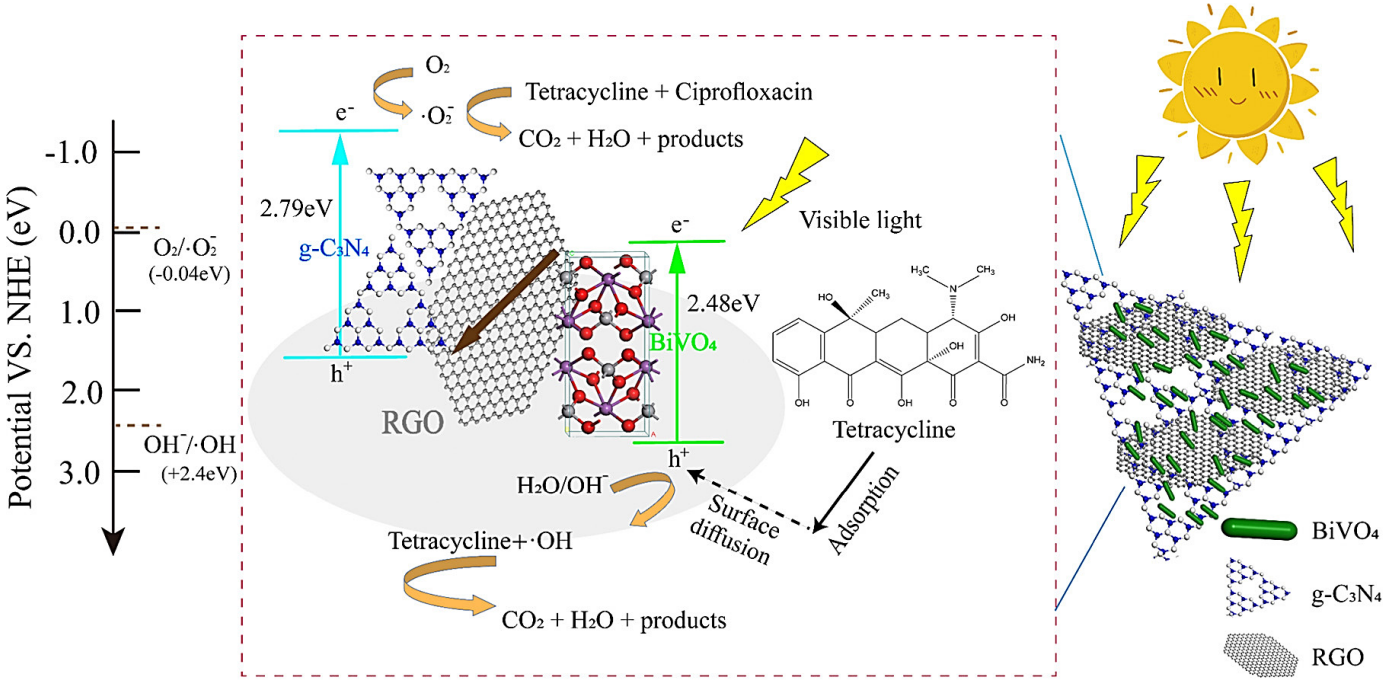

Figure 3. The proposed mechanism for antibiotic photodegradation (tetracycline and ciprofloxacin) using $BiVO_4$/reduced graphene oxide (RGO)/g-C_3N_4 Z-scheme photocatalysts. Adapted from [73] with permission. Copyright 2022 Elsevier.

4. Conclusions and Perspectives

$BiVO_4$ as a narrow-band-gap semiconductor has shown excellent optical features, non-toxicity, and significant chemical stability. $BiVO_4$ nanomaterials with attractive photocatalytic performances have been widely explored for the degradation of dye pollutants and

pharmaceutical wastes as well as for photocatalytic antibacterial applications. Their photocatalytic activity is related to their band gap, particle size, and crystalline phase. Notably, the pH value, morphology, and crystalline phase with significant effects on photocatalytic activities of $BiVO_4$ nanomaterials ought to be further explored. Future explorations should focus on the associated photocatalytic mechanisms and optimization of reaction/synthesis conditions. A wide variety of biosynthesis techniques have been introduced for the synthesis of nanocatalysts with the added benefits of safety, inexpensiveness, simplicity, and environmentally-benign properties. However, additional efforts are still required pertaining to their large-scale/commercial production, optimized reaction/synthesis conditions, stability of the ensued NPs, size distribution, and the adequate control of size/morphology. In this context, understanding the related metabolic pathways, reducing/capping agents, and understanding the underlying mechanisms can help to better control the properties of NPs.

Author Contributions: H.Q.A., writing—review; S.I. and R.S.V., conceptualization, writing—review, and editing. All authors have read and agreed to the published version of the manuscript.

Funding: This research received no external funding.

Institutional Review Board Statement: Not applicable.

Informed Consent Statement: Not applicable.

Data Availability Statement: Not applicable.

Conflicts of Interest: There is no conflict of interest.

References

1. Mohan, R. Green bismuth. *Nat. Chem.* **2010**, *2*, 336. [CrossRef] [PubMed]
2. Salvador, J.A.; Figueiredo, S.A.; Pinto, R.M.; Silvestre, S.M. Bismuth compounds in medicinal chemistry. *Future Med. Chem.* **2012**, *4*, 1495–1523. [CrossRef] [PubMed]
3. Aguilera-Ruiz, E.; Zambrano-Robledo, P.; Vazquez-Arenas, J.; Cruz-Ortiz, B.; Peral, J.; García-Pérez, U.M. Photoactivity of nanostructured spheres of $BiVO_4$ synthesized by ultrasonic spray pyrolysis at low temperature. *Mater. Res. Bull.* **2021**, *143*, 111447. [CrossRef]
4. Koventhan, C.; Pandiyarajan, S.; Chen, S.-M. Simple sonochemical synthesis of flake-ball shaped bismuth vanadate for voltammetric detection of furazolidone. *J. Alloys Compd.* **2022**, *895*, 162315. [CrossRef]
5. Packiaraj, R.; Devendran, P.; Asath Bahadur, S.; Nallamuthu, N. Structural and electrochemical studies of Scheelite type $BiVO_4$ nanoparticles: Synthesis by simple hydrothermal method. *J. Mater. Sci. Mater. Electron.* **2018**, *29*, 13265–13276. [CrossRef]
6. Liu, X.; Xiao, M.; Xu, L.; Miao, Y.; Ouyang, R. Characteristics, applications and determination of bismuth. *J. Nanosci. Nanotechnol.* **2016**, *16*, 6679–6689. [CrossRef]
7. Zhang, A.; Zhang, J. Hydrothermal processing for obtaining of $BiVO_4$ nanoparticles. *Mater. Lett.* **2009**, *63*, 1939–1942. [CrossRef]
8. Trinh, D.T.T.; Khanitchaidecha, W.; Channei, D.; Nakaruk, A. Synthesis, characterization and environmental applications of bismuth vanadate. *Res. Chem. Intermed.* **2019**, *45*, 5217–5259. [CrossRef]
9. Zhao, Z.; Li, Z.; Zou, Z. Electronic structure and optical properties of monoclinic clinobisvanite $BiVO_4$. *Phys. Chem. Chem. Phys.* **2011**, *13*, 4746–4753. [CrossRef]
10. Pookmanee, P.; Kojinok, S.; Puntharod, R.; Sangsrichan, S.; Phanichphant, S. Preparation and characterization of $BiVO_4$ powder by the sol-gel method. *Ferroelectrics* **2013**, *456*, 45–54. [CrossRef]
11. Josephine, A.J.; Dhas, C.R.; Venkatesh, R.; Arivukarasan, D.; Christy, A.J.; Monica, S.E.S.; Keerthana, S. Effect of pH on visible-light-driven photocatalytic degradation of facile synthesized bismuth vanadate nanoparticles. *Mater. Res. Express* **2020**, *7*, 015036. [CrossRef]
12. Xu, H.; Zeiger, B.W.; Suslick, K.S. Sonochemical synthesis of nanomaterials. *Chem. Soc. Rev.* **2013**, *42*, 2555–2567. [CrossRef] [PubMed]
13. Liu, W.; Cao, L.; Su, G.; Liu, H.; Wang, X.; Zhang, L. Ultrasound assisted synthesis of monoclinic structured spindle $BiVO_4$ particles with hollow structure and its photocatalytic property. *Ultrason. Sonochem.* **2010**, *17*, 669–674. [CrossRef] [PubMed]
14. Nguyen, T.D.; Hong, S.-S. Facile solvothermal synthesis of monoclinic-tetragonal heterostructured $BiVO_4$ for photodegradation of rhodamine B. *Catal. Commun.* **2020**, *136*, 105920. [CrossRef]
15. Venkatesan, R.; Velumani, S.; Ordon, K.; Makowska-Janusik, M.; Corbel, G.; Kassiba, A. Nanostructured bismuth vanadate ($BiVO_4$) thin films for efficient visible light photocatalysis. *Mater. Chem. Phys.* **2018**, *205*, 325–333. [CrossRef]
16. Nath, D.; Banerjee, P. Green nanotechnology—A new hope for medical biology. *Environ. Toxicol. Pharmacol.* **2013**, *36*, 997–1014. [CrossRef]

17. Iravani, S.; Varma, R.S. Biofactories: Engineered nanoparticles via genetically engineered organisms. *Green Chem.* **2019**, *21*, 4583–4603. [CrossRef]
18. Iravani, S.; Varma, R.S. Sustainable synthesis of cobalt and cobalt oxide nanoparticles and their catalytic and biomedical applications. *Green Chem.* **2020**, *22*, 2643–2661. [CrossRef]
19. Iravani, S.; Varma, R.S. Greener synthesis of lignin nanoparticles and their applications. *Green Chem.* **2020**, *22*, 612–636. [CrossRef]
20. Iravani, S.; Varma, R.S. Green synthesis, biomedical and biotechnological applications of carbon and graphene quantum dots. A review. *Environ. Chem. Lett.* **2020**, *18*, 703–727. [CrossRef]
21. Ngullie, R.C.; Alaswad, S.O.; Bhuvaneswari, K.; Shanmugam, P.; Pazhanivel, T.; Arunachalam, P. Synthesis and Characterization of Efficient ZnO/g-C_3N_4 Nanocomposites Photocatalyst for Photocatalytic Degradation of Methylene Blue. *Coatings* **2020**, *10*, 500. [CrossRef]
22. Nasrollahzadeh, M.; Sajjadi, M.; Iravani, S.; Varma, R.S. Trimetallic Nanoparticles: Greener Synthesis and Their Applications. *Nanomaterials* **2020**, *10*, 1784. [CrossRef] [PubMed]
23. Nasrollahzadeh, M.; Sajjadi, M.; Iravani, S.; Varma, R.S. Green-synthesized nanocatalysts and nanomaterials for water treatment: Current challenges and future perspectives. *J. Hazard. Mater.* **2021**, *401*, 123401. [CrossRef] [PubMed]
24. Khatami, M.; Iravani, S. Green and eco-friendly synthesis of nanophotocatalysts: An overview. *Comments Inorg. Chem.* **2021**, *41*, 133–187. [CrossRef]
25. Tammina, S.K.; Mandal, B.K.; Kadiyala, N.K. Photocatalytic degradation of methylene blue dye by nonconventional synthesized SnO_2 nanoparticles. *Environ. Nanotechnol. Monit. Manag.* **2018**, *10*, 339–350. [CrossRef]
26. Mahanthappa, M.; Kottam, N.; Yellappa, S. Enhanced photocatalytic degradation of methylene blue dye using CuSCdS nanocomposite under visible light irradiation. *Appl. Surf. Sci.* **2019**, *475*, 828–838. [CrossRef]
27. Paul, A.; Dhar, S.S. Construction of hierarchical $MnMoO_4/NiFe_2O_4$ nanocomposite: Highly efficient visible light driven photocatalyst in the degradation of different polluting dyes in aqueous medium. *Colloids Surf. A Physicochem. Eng. Asp.* **2020**, *585*, 124090. [CrossRef]
28. Fatima, U.; Khalid, N.R.; Nawaz, T.; Tahir, M.B.; Fatima, N.; Kebaili, I.; Alrobei, H.; Alzaid, M.; Shahzad, K.; Ali, A.M. Synthesis of $BiVO_4/NiFe_2O_4$ composite for photocatalytic degradation of methylene blue. *Appl. Nanosci.* **2021**, *11*, 2793–2800. [CrossRef]
29. Lee, G.-J.; Lee, X.-Y.; Lyu, C.; Liu, N.; Andandan, S.; Wu, J.J. Sonochemical Synthesis of Copper-doped $BiVO_4$/g-C_3N_4 Nanocomposite Materials for Photocatalytic Degradation of Bisphenol A under Simulated Sunlight Irradiation. *Nanomaterials* **2020**, *10*, 498. [CrossRef]
30. Letchumanan, D.; Sok, S.P.; Ibrahim, S.; Nagoor, N.H.; Arshad, N.M. Plant-Based Biosynthesis of Copper/Copper Oxide Nanoparticles: An Update on Their Applications in Biomedicine, Mechanisms, and Toxicity. *Biomolecules* **2021**, *11*, 564. [CrossRef]
31. Pasula, R.R.; Lim, S. Engineering nanoparticle synthesis using microbial factories. *Eng. Biol.* **2017**, *1*, 12–17. [CrossRef]
32. Luo, C.-H.; Shanmugam, V.; Yeh, C.-S. Nanoparticle biosynthesis using unicellular and subcellular supports. *NPG Asia Mater.* **2015**, *7*, e209. [CrossRef]
33. Varma, R.S. Greener approach to nanomaterials and their sustainable applications. *Curr. Opin. Chem. Eng.* **2012**, *1*, 123–128. [CrossRef]
34. Varma, R.S. Journey on greener pathways: From the use of alternate energy inputs and benign reaction media to sustainable applications of nano-catalysts in synthesis and environmental remediation. *Green Chem.* **2014**, *16*, 2027–2041. [CrossRef]
35. Varma, R.S. Greener and sustainable chemistry. *Appl. Sci.* **2014**, *4*, 493–497. [CrossRef]
36. Varma, R.S. Greener and Sustainable Trends in Synthesis of Organics and Nanomaterials. *ACS Sustain. Chem. Eng.* **2016**, *4*, 5866–5878. [CrossRef]
37. Karatoprak, G.Ş.; Aydin, G.; Altinsoy, B.; Altinkaynak, C.; Koşar, M.; Ocsoy, I. The Effect of Pelargonium endlicherianum Fenzl. root extracts on formation of nanoparticles and their antimicrobial activities. *Enzym. Microb. Technol.* **2017**, *97*, 21–26. [CrossRef]
38. Pramila, S.; Nagaraju, G.; Mallikarjunaswamy, C.; Latha, K.; Chandan, S.; Ramu, R.; Rashmi, V.; Lakshmi Ranganatha, V. Green Synthesis of $BiVO_4$ nanoparticles by microwave method using *Aegle marmelos* juice as a fuel: Photocatalytic and antimicrobial study. *Anal. Chem. Lett.* **2020**, *10*, 298–306. [CrossRef]
39. Mohamed, H.; Sone, B.; Khamlich, S.; Coetsee-Hugo, E.; Swart, H.; Thema, T.; Sbiaa, R.; Dhlamini, M. Biosynthesis of $BiVO_4$ nanorods using Callistemon viminalis extracts: Photocatalytic degradation of methylene blue. *Mater. Today Proc.* **2021**, *36*, 328–335. [CrossRef]
40. Baliga, M.S.; Shivashankara, A.R.; Haniadka, R.; Dsouza, J.; Bhat, H.P. Phytochemistry, nutritional and pharmacological properties of *Artocarpus heterophyllus* Lam (jackfruit): A review. *Food Res. Int.* **2011**, *44*, 1800–1811. [CrossRef]
41. Mallikarjunaswamy, C.; Pramila, S.; Nagaraju, G.; Ramu, R.; Ranganatha, V.L. Green synthesis and evaluation of antiangiogenic, photocatalytic, and electrochemical activities of $BiVO_4$ nanoparticles. *J. Mater. Sci. Mater. Electron.* **2021**, *32*, 14028–14046. [CrossRef]
42. Manjunatha, A.S.; Pavithra, N.S.; Marappa, S.; Prashanth, S.A.; Nagaraju, G. Green synthesis of flower-like $BiVO_4$ nanoparticles by solution combustion method using lemon (*Citrus limon*) juice as a fuel: Photocatalytic and electrochemical study. *ChemistrySelect* **2018**, *3*, 13456–13463. [CrossRef]
43. Farag, M.A.; Paré, P.W. Phytochemical analysis and anti-inflammatory potential of *Hyphaene thebaica* L. fruit. *J. Food Sci.* **2013**, *78*, C1503–C1508. [CrossRef] [PubMed]

44. Mohamed, H.E.A.; Afridi, S.; Khalil, A.T.; Zohra, T.; Alam, M.M.; Ikram, A.; Shinwari, Z.K.; Maaza, M. Phytosynthesis of $BiVO_4$ nanorods using *Hyphaene thebaica* for diverse biomedical applications. *AMB Express* **2019**, *9*, 200. [CrossRef] [PubMed]
45. Bhardwaj, R.; Nandal, U. Nutritional and therapeutic potential of bael (*Aegle marmelos* Corr.) fruit juice: A review. *Nutr. Food Sci.* **2015**, *45*, 895–919. [CrossRef]
46. Burakova, E.A.; Dyachkova, T.P.; Rukhov, A.V.; Tugolukov, E.N.; Galunin, E.V.; Tkachev, A.G.; Basheer, A.A.; Ali, I. Novel and economic method of carbon nanotubes synthesis on a nickel magnesium oxide catalyst using microwave radiation. *J. Mol. Liq.* **2018**, *253*, 340–346. [CrossRef]
47. Kumar, A.; Kuang, Y.; Liang, Z.; Sun, X. Microwave chemistry, recent advancements, and eco-friendly microwave-assisted synthesis of nanoarchitectures and their applications: A review. *Mater. Today Nano* **2020**, *11*, 100076. [CrossRef]
48. Chen, M.; Chen, C.; Shi, S.; Chen, C. Low-temperature synthesis multiwalled carbon nanotubes by microwave plasma chemical vapor deposition using CH_4–CO_2 gas mixture. *Jpn. J. Appl. Phys.* **2003**, *42*, 614–619. [CrossRef]
49. Daniel Abraham, S.; Theodore David, S.; Biju Bennie, R.; Joel, C.; Sanjay Kumar, D. Eco-friendly and green synthesis of $BiVO_4$ nanoparticle using microwave irradiation as photocatalayst for the degradation of Alizarin Red S. *J. Mol. Struct.* **2016**, *1113*, 174–181. [CrossRef]
50. Claudino, C.H.; Kuznetsova, M.; Rodrigues, B.S.; Chen, C.; Wang, Z.; Sardela, M.; Souza, J.S. Facile one-pot microwave-assisted synthesis of tungsten-doped $BiVO_4/WO_3$ heterojunctions with enhanced photocatalytic activity. *Mater. Res. Bull.* **2020**, *125*, 110783. [CrossRef]
51. Zhang, Y.; Li, G.; Yang, X.; Yang, H.; Lu, Z.; Chen, R. Monoclinic $BiVO_4$ micro-/nanostructures: Microwave and ultrasonic wave combined synthesis and their visible-light photocatalytic activities. *J. Alloys Compd.* **2013**, *551*, 544–550. [CrossRef]
52. Souza, J.S.; Hirata, F.T.H.; Corio, P. Microwave-assisted synthesis of bismuth vanadate nanoflowers decorated with gold nanoparticles with enhanced photocatalytic activity. *J. Nanopart. Res.* **2019**, *21*, 35. [CrossRef]
53. Pingmuang, K.; Nattestad, A.; Kangwansupamonkon, W.; Wallace, G.G.; Phanichphant, S.; Chen, J. Phase-controlled microwave synthesis of pure monoclinic $BiVO_4$ nanoparticles for photocatalytic dye degradation. *Appl. Mater. Today* **2015**, *1*, 67–73. [CrossRef]
54. Rodrigues, B.S.; Branco, C.M.; Corio, P.; Souza, J.S. Controlling Bismuth Vanadate Morphology and Crystalline Structure through Optimization of Microwave-Assisted Synthesis Conditions. *Cryst. Growth Des.* **2020**, *20*, 3673–3685. [CrossRef]
55. Kansaard, T.; Bangbai, C.; Jayasankar, C.K.; Pecharapa, W. Effect of Ultrasonic Irradiation Time on Physical Properties and Photocatalytic Performance of $BiVO_4$ Nanoparticles Prepared via Sonochemical Process. *Integr. Ferroelectr.* **2021**, *214*, 123–132. [CrossRef]
56. Tahir, M.B.; Iqbal, T.; Kiran, H.; Hasan, A. Insighting role of reduced graphene oxide in $BiVO_4$ nanoparticles for improved photocatalytic hydrogen evolution and dyes degradation. *Int. J. Energy Res.* **2019**, *43*, 2410–2417. [CrossRef]
57. Walsh, A.; Yan, Y.; Huda, M.N.; Al-Jassim, M.M.; Wei, S.-H. Band Edge Electronic Structure of $BiVO_4$: Elucidating the Role of the Bi s and V d Orbitals. *Chem. Mater.* **2009**, *21*, 547–551. [CrossRef]
58. Lai, B.-R.; Lin, L.-Y.; Xiao, B.-C.; Chen, Y.-S. Facile synthesis of bismuth vanadate/bismuth oxide heterojunction for enhancing visible light-responsive photoelectrochemical performance. *J. Taiwan Inst. Chem. Eng.* **2019**, *100*, 178–185. [CrossRef]
59. Reddy, C.V.; Reddy, I.N.; Koutavarapu, R.; Reddy, K.R.; Kim, D.; Shim, J. Novel $BiVO_4$ nanostructures for environmental remediation, enhanced photoelectrocatalytic water oxidation and electrochemical energy storage performance. *Sol. Energy* **2020**, *207*, 441–449. [CrossRef]
60. Sajid, M.M.; Amin, N.; Shad, N.A.; Bashir khan, S.; Javed, Y.; Zhang, Z. Hydrothermal fabrication of monoclinic bismuth vanadate (m-$BiVO_4$) nanoparticles for photocatalytic degradation of toxic organic dyes. *Mater. Sci. Eng. B* **2019**, *242*, 83–89. [CrossRef]
61. Ganeshbabu, M.; Kannan, N.; Sundara Venkatesh, P.; Paulraj, G.; Jeganathan, K.; MubarakAli, D. Synthesis and characterization of $BiVO_4$ nanoparticles for environmental applications. *RSC Adv.* **2020**, *10*, 18315–18322. [CrossRef] [PubMed]
62. Sharma, R.; Uma; Singh, S.; Verma, A.; Khanuja, M. Visible light induced bactericidal and photocatalytic activity of hydrothermally synthesized $BiVO_4$ nano-octahedrals. *J. Photochem. Photobiol. B Biol.* **2016**, *162*, 266–272. [CrossRef] [PubMed]
63. Lopes, O.F.; Carvalho, K.T.; Macedo, G.K.; de Mendonca, V.R.; Avansi, W.; Ribeiro, C. Synthesis of BiVO 4 via oxidant peroxo-method: Insights into the photocatalytic performance and degradation mechanism of pollutants. *New J. Chem.* **2015**, *39*, 6231–6237. [CrossRef]
64. Dowla Biswas, M.R.U.; Ho, B.S.; Oh, W.-C. Eco-friendly conductive polymer-based nanocomposites, $BiVO_4$/graphene oxide/polyaniline for excellent photocatalytic performance. *Polym. Bull.* **2020**, *77*, 4381–4400. [CrossRef]
65. Tahir, M.B.; Riaz, K.N.; Asiri, A.M. Boosting the performance of visible light-driven WO_3/g-C_3N_4 anchored with $BiVO_4$ nanoparticles for photocatalytic hydrogen evolution. *Int. J. Energy Res.* **2019**, *43*, 5747–5758. [CrossRef]
66. Dhabarde, N.; Carrillo-Ceja, O.; Tian, S.; Xiong, G.; Raja, K.; Subramanian, V.R. Bismuth Vanadate Encapsulated with Reduced Graphene Oxide: A Nanocomposite for Optimized Photocatalytic Hydrogen Peroxide Generation. *J. Phys. Chem. C* **2021**, *125*, 23669–23679. [CrossRef]
67. Kansaard, T.; Pecharapa, W. Characterization of $BiVO_4$ nanoparticles prepared by sonochemical process. *Ferroelectrics* **2019**, *552*, 140–147. [CrossRef]
68. Tian, H.; Wu, H.; Fang, Y.; Li, R.; Huang, Y. Hydrothermal synthesis of m-$BiVO_4$/t-$BiVO_4$ heterostructure for organic pollutants degradation: Insight into the photocatalytic mechanism of exposed facets from crystalline phase controlling. *J. Hazard. Mater.* **2020**, *399*, 123159. [CrossRef]

69. Jiang, H.; Dai, H.; Meng, X.; Zhang, L.; Deng, J.; Liu, Y.; Au, C.T. Hydrothermal fabrication and visible-light-driven photocatalytic properties of bismuth vanadate with multiple morphologies and/or porous structures for Methyl Orange degradation. *J. Environ. Sci.* **2012**, *24*, 449–457. [CrossRef]
70. Choe, H.R.; Kim, J.H.; Ma, A.; Jung, H.; Kim, H.Y.; Nam, K.M. Understanding Reaction Kinetics by Tailoring Metal Co-catalysts of the $BiVO_4$ Photocatalyst. *ACS Omega* **2019**, *4*, 16597–16602. [CrossRef]
71. Ma, Y.; Pendlebury, S.R.; Reynal, A.; Formal, F.L.; Durrant, J.R. Dynamics of photogenerated holes in undoped $BiVO_4$ photoanodes for solar water oxidation. *Chem. Sci.* **2014**, *5*, 2964–2973. [CrossRef]
72. Yan, Y.; Sun, S.; Song, Y.; Yan, X.; Guan, W.; Liu, X.; Shi, W. Microwave-assisted in situ synthesis of reduced graphene oxide-$BiVO_4$ composite photocatalysts and their enhanced photocatalytic performance for the degradation of ciprofloxacin. *J. Hazard. Mater.* **2013**, *250–251*, 106–114. [CrossRef] [PubMed]
73. Li, Z.; Bao, Z.; Yao, F.; Cao, H.; Wang, J.; Qiu, L.; Lv, J.; Sun, X.; Zhang, Y.; Wu, Y. One-dimensional bismuth vanadate nanostructures constructed Z-scheme photocatalyst for highly efficient degradation of antibiotics. *J. Water Process Eng.* **2022**, *46*, 102599. [CrossRef]
74. Hemavibool, K.; Sansenya, T.; Nanan, S. Enhanced Photocatalytic Degradation of Tetracycline and Oxytetracycline Antibiotics by BiVO4 Photocatalyst under Visible Light and Solar Light Irradiation. *Antibiotics* **2022**, *11*, 761. [CrossRef]